Computers Math. Applic. Vol. 25, No. 2, pp. 59–72, 1993
Printed in Great Britain.

0097-4943/93 $5.00 + 0.00

A MULTIDISCIPLINARY OPTIMIZATION APPROACH FOR VIBRATION REDUCTION IN HELICOPTER ROTOR BLADES

ADITI CHATTOPADHYAY AND THOMAS R. MCCARTHY
Department of Mechanical and Aerospace Engineering
Arizona State University, Tempe, Arizona 85287-6106, U.S.A.

(Received February 1992)

Abstract—The paper addresses the integration of blade dynamics, aerodynamics, structures and aeroelasticity in the design of helicopter rotors using a formal optimization technique. The interaction of the disciplines is studied inside a closed-loop optimization process. The goal is to reduce vibratory shear forces at the blade root with constraints imposed on dynamic, structural and aeroelastic design requirements. Both structural and aerodynamic design variables are used. Multiobjective formulation procedures are needed since more than one design objective is used. A nonlinear programming technique and an approximate analysis procedure are used for optimization. Substantial reductions are obtained in the vibratory root forces and moments while satisfying the remaining design criteria. The results of the optimization procedure using two multiobjective formulation procedures, are compared with a baseline or reference design.

NOMENCLATURE

c	chord, ft
f_r	3/rev radial shear, lb
f_x	3/rev inplane shear, lb
f_z	4/rev vertical shear, lb
g_1, g_2	constraint functions
m_c	3/rev torsional moment, lb-ft
m_x	3/rev flapping moment, lb-ft
m_z	4/rev lagging moment, lb-ft
$\bar{m}_z, \bar{f}_z$	prescribed values of m_z and f_z, respectively
m_{z_0}, f_{z_0}	values of m_z and f_z at the beginning of an iteration
p	chord distribution shape parameter
t_i	box beam wall thicknesses, ft
w_{t_j}	leading edge nonstructural weight at j^{th} node, lb
w_{c_j}	central nonstructural weight at j^{th} node, lb
x_e	center of gravity offset forward of shear center
x, y, z	reference axes
$\bar{y}$	nondimensional radial location
AI	autorotational inertia, lb-ft^2
C_T	thrust coefficient
C_p	power coefficient
F_1, F_2	objective functions
K	total number of constraints and objective functions
NCON	number of constraints
NDV	number of design variables
NOBJ	number of objective functions
NSEG	number of blade segments
NMEM	number of box beam structural members
R	blade radius, ft
T	thrust, lb
W	total blade weight, lb
α	chord distribution shape parameter
β_1, β_2	pseudo design variables
δ	twist shape parameter
λ	inverse taper ratio
μ	advance ratio
ϕ_i	i^{th} design variable
ρ	K-S function multiplier
θ	blade twist, degrees
σ	area-weighted solidity
σ_{T_j}	total blade stress, at the j^{th} segment
τ	twist ratio
Ω	rotor angular velocity, rad/sec

Subscripts

al	allowable value
max	maximum value
r	value at the blade root
ref	reference blade value
t	value at the blade tip
L	lower bound
U	upper bound

INTRODUCTION

An emerging trend in the design of aerospace vehicles is the integration of multidisciplinary analysis inside an optimum design process [1]. This means that designs are to be obtained by

accounting for the interactions between the appropriate disciplines simultaneously and not sequentially. The design of a helicopter, particularly the rotor, is a perfect example where integrated design optimization is an essential tool.

Although there has been a great deal of interest in optimal design of rotorcraft, most of the researchers addressed the problem in a sequential manner, based on individual disciplines, and attempts were made to satisfy certain design requirements and criteria related to a single discipline [2–9]. Since vibration has long been a major problem in helicopters, a majority of the research efforts have addressed this issue. For a helicopter in forward flight, the largest component of the airframe vibratory forces occur at the fundamental blade passing frequency, $n\Omega$, where n represents the number of blades and Ω is the rotor r.p.m. This involves consideration of the rotor responses to airloads at $n \pm 1$ harmonics as well. It is also important to separate the natural frequencies of the blade from the harmonics of the airloads to avoid resonance. Therefore, reducing helicopter vibration by attacking the source, namely the blade, is an attractive concept and has been addressed by many researchers. An early review of the literature in the area of application of optimum design techniques with dynamic constraints is due to Friedmann [2] and Miura [3]. In the majority of the work dealing with optimum blade designs for reduced vibration, the blades were either considered to be in a vacuum [4–7] or a simple forced response analysis was performed. In cases where rotor analysis was used, quasi-steady airloads were used and the effects of the design changes, during optimization, on changes in the blade airloads were not included [8–11].

Discipline-based design procedures are not only time consuming, but can also lead to a final design that may not be an optimum solution with respect to the sequential designs. For example, in an effort to reduce vibration when the mass and stiffness distributions of the blade are changed, spanwise and/or chordwise, it is important to ensure that the aeroelastic stability of the rotor is not degraded. This further complicates the design problem, since a proper formulation requires the coupling of a comprehensive aeroelastic analysis procedure, along with other analyses, inside the optimization loop. The rotor blade aerodynamic design process consists of the selection of variables such as blade planform, airfoils, twist, and tip shape. The process is further complicated by the often conflicting requirements between forward flight and hover. As indicated by Magee *et al.* [12], the *best* twist for hover produces a negative angle of attack on inboard airfoil sections in forward flight conditions, whereas the *best* twist in forward flight causes the blade to stall inboard in hover. Similar conflict also occurs in the choice of the chord distribution. Therefore, it is necessary to merge the appropriate disciplines to obtain an integrated design procedure.

Due to the importance of the problem, some initial investigations with partial integration of some of the disciplines have been reported [13–18]. A first investigation of integrated aerodynamic load/dynamic optimization was presented by Chattopadhyay *et al.* [13]. The 4/rev vertical shear was minimized along with the blade weight using a multiobjective formulation called the "Global Criteria Approach." Constraints were imposed on elastic coupled lead-lag and flapping dominated frequencies, blade autorotational inertia and centrifugal stress. Design variables included blade stiffnesses at the root, nonstructural weights (located spanwise), taper ratio, root chord, and radius of gyration at the blade root. The integration of aerodynamic loads and dynamics was achieved by coupling a comprehensive helicopter analysis code, CAMRAD [19] to an optimizer comprising CONMIN [20] and an approximate analysis technique. The use of the program CAMRAD permitted the design of the blade with calculated airloads, and its presence in the closed loop optimization procedure allowed the inclusion of the effects due to changes in these airloads with changes in design variables. Chattopadhyay and Chiu [14] extended the work in [13] to include the remaining critical vibratory forces and moments, in the form of objective functions and/or constraints, to arrive at a more comprehensive formulation. Most importantly, to ensure that the optimized rotor maintains the same lifting capability as the reference rotor, an additional constraint was imposed on the total thrust.

A combined structural, dynamic and aerodynamic optimization of rotor blades was addressed by He and Peters [15]. He and Peters used a single-cell box beam model to represent the structural component in the blade and the blade performance was optimized using the power required in hover as the objective function. Constraints were imposed on natural frequencies, blade stress, and fatigue life. The optimization problem was addressed sequentially, the hover performance

was improved first and the frequency placements were performed at a lower level. The optimization was performed with an assumed blade loading. Weller and Davis [16] applied optimization techniques to reduce vibratory loads by incorporating constraints on the structural damping and natural frequencies. A simplified rotor analysis code which used quasi-steady airloads was used. More recently, Straub *et al.* [17] addressed the problem of combined performance/vibration optimization by using a comprehensive rotor analysis code. A linear combination was used for the multiple design objective problem. Chattopadhyay and McCarthy [18] recently addressed the issue of proper choice of multiobjective formulation procedures in the context of a nonlinear rotor blade optimization problem. The optimum design problem of [14] was solved using three different multiobjective formulation techniques, the modified "Global Criterion Approach," the "Minimum Sum Beta" (Min $\Sigma\beta$) approach [16] and the Kreisselmeier-Steinhauser (K-S) function approach [21].

In the present paper, a further step towards the completely integrated optimization procedure for a rotor blade is taken by incorporating rotor structural, dynamic, aerodynamic, and aeroelastic stability requirements in the optimization formulation, in the presence of actual air loads. A detailed structural model is used inside the airfoil and the generic design variables such as stiffnesses, used in [13,14,18], are replaced by structural geometric variables such as wall thicknesses. In addition, planform design variables, such as taper, and aerodynamic design variables, such as chord and twist distributions, are also used to study the trade-off between dynamic and aerodynamic performance requirements. The linear chord variation used in the previous work [13,14,18] is replaced by a more realistic nonlinear chord distribution. This provides more flexibility to the optimization process by introducing additional design variables. The multiobjective optimization problem is formulated using both the Min $\Sigma\beta$ and K-S function approaches. The results obtained using these techniques are described and a comparison of the two methods is presented.

OPTIMIZATION PROBLEM

The optimization problem can be mathematically posed as follows:

Minimize

$$F_k(\varphi_n); \qquad k = 1,2,\ldots,\text{NOBJ}, \qquad n = 1,2,\ldots,\text{NDV}, \qquad \text{Objective functions,}$$

subject to

$$g_j(\varphi_n) \leq 0; \qquad j = 1,2,\ldots,\text{NCON}, \qquad \text{Inequality constraints,}$$

$$\varphi_{n_L} \leq \varphi_n \leq \varphi_{n_U}; \qquad \text{Side constraints,}$$

where NOBJ denotes the number of objective functions, NDV is the number of design variables and NCON is the total number of constraints. The subscripts L and U denote lower and upper bounds, respectively, on the design variable φ. In this paper, since a multidisciplinary design problem is addressed, the objective functions, the constraints and the design variables are carefully selected from each of the disciplines considered. A detailed description of the baseline or the "reference blade," and a description of the various discipline based design criteria are described next.

Blade Model

The reference blade chosen for this study is a modified wind tunnel model of an advanced articulated rotor blade of the Growth Black Hawk type [22]. The load carrying structure of the rotor is modeled as a double-celled box beam that is symmetric about the x-axis (Figure 1). The outer dimensions of the box beam are constants based on the chord. The individual thicknesses of the webs and the flanges are linearly varied with the chord such that

$$t_i(y) = t_{i_r} \frac{c(y)}{c_r}, \tag{1}$$

where t_i, is the thickness of the i^{th} wall of the box beam ($i = 1,2,\ldots,$NMEM), c is the chord and the subscript r refers to values at the blade root. Nonstructural tuning masses are placed at the center of the rectangular cell (w_c) and at the leading edge (w_l).

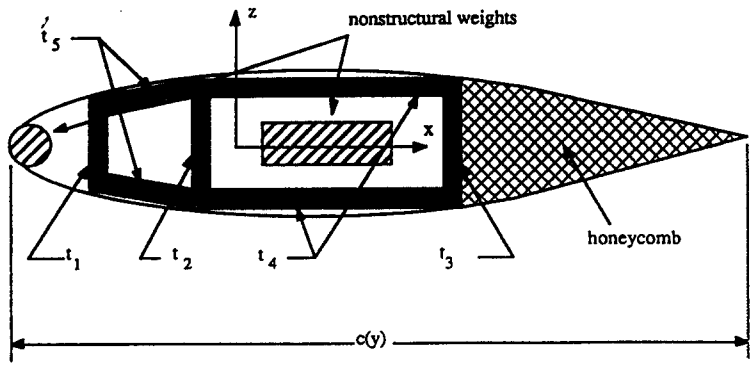

Figure 1. Double-celled box beam configuration

Chord Distribution

The normalized chord distribution, $\bar{c}(y)$, is defined to have spanwise chord variation as follows

$$\bar{c}(y) = \frac{c(y)}{c_r} = [1 + \bar{y}(\lambda - 1)]\,[1 - \bar{y}^{1/\alpha}]^p, \tag{2}$$

where c_r is the root chord, $\bar{y}$ is the nondimensional radius and λ is the inverse taper ratio, i.e., $\lambda = c_t/c_r$, where c_t is the tip chord. Note that $\lambda = 0$ yields a triangular blade planform. The tip shape parameter is denoted p and defines the blade shape at the tip. The tip length parameter is denoted α and defines the amount of tip taper. Both of these parameters are defined to be positive and their physical significance is illustrated in Figures 2 and 3.

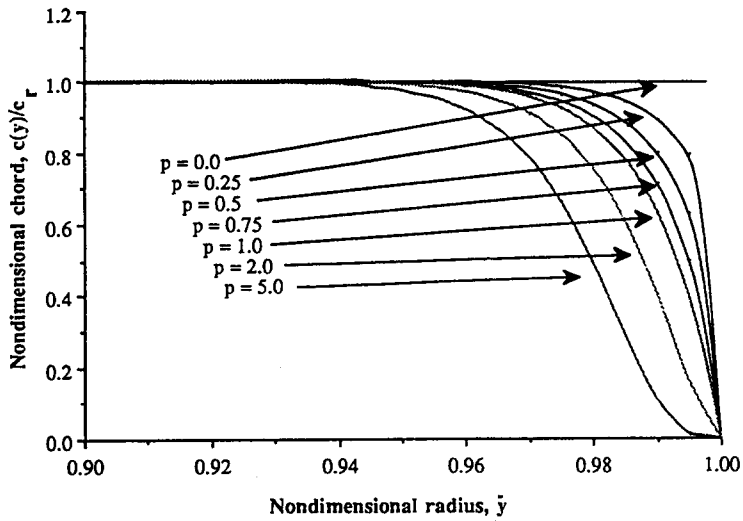

Figure 2. Variation of tip shape with tip shape parameter p, $\alpha = 0.001$ and $\lambda = 1.0$.

Twist Distribution

The twist angle of attack, $\bar{\theta}(y)$, normalized with respect to the root twist θ_r, is defined to have the following spanwise variation

$$\bar{\theta}(y) = \frac{\theta(y)}{\theta_r} = 1 + \bar{y}^{\delta}(\tau - 1). \tag{3}$$

In the above equation, τ is the twist ratio, given by $\tau = \theta_t/\theta_r$, where θ_t is the tip twist, and δ is the twist shape parameter which is defined to be positive. The physical significance of the twist ratio, τ, is shown in Figure 4 which indicates that when $0 < \tau < 1$ the twist is concave, and similarly when $\tau > 1$ the twist is convex. The limiting case of $\tau = 1$ indicates linear twist.

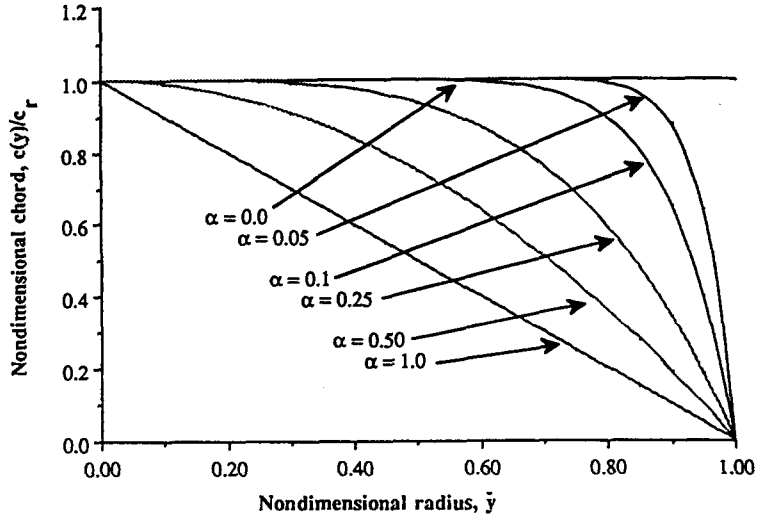

Figure 3. Variation of chord with tip length parameter α, $p = 1.0$ and $\lambda = 1.0$.

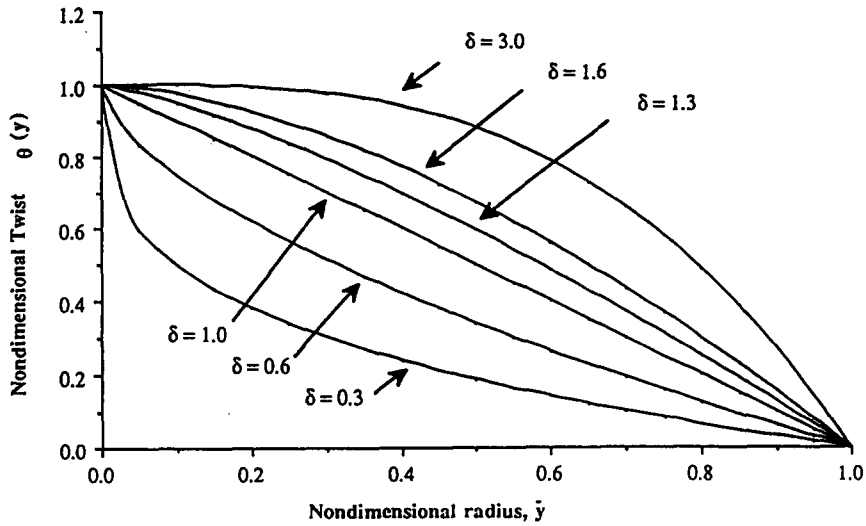

Figure 4. Variation of blade twist with changes in twist parameter, δ, ($\tau = 0.0$).

Dynamic Criteria

In this paper, the optimum design of the rotor blade under forward flight condition is addressed with the objectives of minimizing the critical vibratory forces and moments at the blade root. The rotor being four-bladed, the 4/rev vertical shear (f_z) and the 4/rev lagging moment (m_z), at the blade root, are used as objective functions. Upper bound constraints are imposed on the remaining critical forces and moments. In previous papers [13,14,18], the authors used windows on the blade natural frequencies to prevent resonance, however, it was determined that these constraints would be included implicitly by constraining the vibratory loads. The following constraints are imposed:

(i) 3/rev radial shear, $f_r \leq f_{r_U}$;
(ii) 3/rev inplane shear, $f_x \leq f_{x_U}$;
(iii) 4/rev flapping moments, $m_x \leq m_{x_U}$;
(iv) 4/rev torsional moments, $m_c \leq m_{c_U}$.

Aerodynamic Criteria

The rotor power required is a measure of economic efficiency, therefore a constraint is imposed on the total power coefficient, C_p, to prevent it from increasing above the baseline value. It is also essential that the optimized rotor retains at least the same lifting capability as the reference

rotor, therefore a lower bound is imposed on the total rotor thrust (T). The constraints are described below:

(v) $C_p \leq C_{p_U}$;
(vi) $T \geq T_L$.

Structural Criteria

Most vibration reduction problems are associated with increased weight, therefore, to avoid such a weight penalty, an upper bound is imposed on the total weight (W) of the blade, where the total weight comprises the structural weight and the nonstructural weight. The blade must also have sufficient autorotational inertia to autorotate in case of engine failure. Therefore, a lower bound is imposed on the autorotational inertia (AI) of the blade. An upper bound (with a factor of safety of 2) is also imposed upon blade stresses to ensure structural integrity. Details of the structural constraints follow:

(vii) $W \leq W_U$;
(viii) $AI \geq AI_L$;
(ix) $\sigma_{T_j} \leq \sigma_{al}$; $j = 1, \ldots, \text{NSEG}$.

Aeroelastic Criteria

Since an articulated rotor is used as a baseline design, a simple constraint on the offset between the shear center and the center of mass of the blade (x_e) can prevent classical bending-torsion flutter. Therefore, the following constraint is imposed:

(x) $x_{e_i} \geq 0$; $i = 1, 2, \ldots, \text{NSEG}$,

i.e., the center of mass must be located forward of the shear center along the span.

Design Variables

For the optimization procedure, both aerodynamic and structural design variables are used in order to give more flexibility to the optimizer. Following, are the design variables used.

(i) Chord distribution parameters, c_r, λ, α, and p;
(ii) Twist distribution parameters, θ_r, τ, and δ;
(iii) Box beam wall thicknesses at the root, t_{i_r}; $i = 1, 2, \ldots, \text{NMEM}$;
(iv) Nonstructural weights, w_{t_j} and w_{c_j}; $j = 1, 2, \ldots, \text{NSEG}$.

ANALYSIS

Dynamic and Aerodynamic Analyses

The program CAMRAD is used for both blade dynamic and aerodynamic analyses. Within CAMRAD, the blade is trimmed at each cycle so that the intermediate designs, which represent feasible designs, are trimmed configurations. A wind tunnel trim option is used, and the rotor lift and drag, each normalized with respect to solidity, and the flapping angle are trimmed using the collective pitch, the cyclic pitch, and the shaft angle. While using this procedure, in the previous studies [13,14,18], the optimized rotor was trimmed to the (C_T/σ) value of the reference blade, where C_T represents the rotor thrust coefficient and σ is the area-weighted solidity of the rotor. This, coupled with the constraint on the total thrust (or C_T), implied that the solidity of the optimized rotor was also constrained to be equal to σ_{ref}, i.e., the reference blade value. To avoid this and allow for σ flexibility, the following trim procedure was implemented in the present paper:

$$\left(\frac{C_T}{\sigma}\right)_{\text{trim}} = \left(\frac{C_T}{\sigma}\right)_{\text{ref}} \left(\frac{\sigma_{\text{ref}}}{\sigma}\right), \tag{4}$$

where σ denotes the current value of the solidity. This allows for the blade, undergoing optimization, to be trimmed at a different value of C_T/σ at each cycle.

Structural Analysis

The structural analysis of the rotor blade was performed using a recently developed inhouse code. The code models a simple two-cell homogeneous box-beam with one rectangular cell and one trapezoidal cell (Figure 1). The beam is symmetrical about the x-axis and is assumed to carry all loads within the rotor. It is assumed that the flatwise, chordwise and torsional stiffnesses of the blade are provided by the box-beam.

OPTIMIZATION PROCEDURE

The optimization algorithm used is the program CONMIN, which is an optimizer based upon the method of feasible directions. Since the use of exact analyses for the calculations of the objective functions and constraints during each iteration of CONMIN is computationally prohibitive, an approximate analysis technique, based upon a first order linear Taylor series approximation, is used.

Multiobjective Optimization Formulation

Due to the fact that the optimization problem involves more than one design objective, the objective function formulation is more complicated than single objective optimization problems. For this study two different multiple objective function formulation techniques are used, the Minimum Sum Beta (Min $\Sigma\beta$) approach and the Kreisselmeier-Steinhauser (K-S) function approach.

Minimum Sum Beta (Min $\Sigma\beta$) Approach

This method, first introduced by Weller and Davis [16], uses the sum of the individual objective function target values (or tolerances) as the overall design objective. The objective function to be minimized, $F_1(\varphi)$, is therefore linear and is defined as follows:

$$F_1(\varphi) = \beta_1 + \beta_2, \tag{5}$$

where β_1 and β_2 are two pseudo design variables with properties such that the original objective functions m_z and f_z remain within $\pm\beta_i$, $(i = 1,2)$ tolerance of these prescribed target values. Using this requirement the constraints are formulated to assume the following form [18]:

$$\frac{m_z - \bar{m}_z}{\bar{m}_z} \leq \beta_1, \tag{6}$$

$$\frac{f_z - \bar{f}_z}{\bar{f}_z} \leq \beta_2, \tag{7}$$

where the quantities $\bar{m}_z$ and $\bar{f}_z$ are the prescribed target values of the objective functions m_z and f_z, respectively, and β_1 and β_2 are the two new 'pseudo' design variables. The design variables for the Min $\Sigma\beta$ formulation, therefore, comprise the original set of design variables and the two pseudo design variables β_1 and β_2. The new constraint vector, $g_{1k}, k = 1,2,\ldots,K$ comprises the original constraints and the two new constraints presented in equations (6) and (7), i.e., $K = \text{NCON} + \text{NOBJ}$.

Kreisselmeier-Steinhauser (K-S) Function Approach

Using this approach, the original objective functions are transformed into reduced objective functions, which assume the following form:

$$m_z^*(\varphi) = \frac{m_z(\varphi)}{m_{z_0}} - 1 - g_{\max} \leq 0, \tag{8}$$

$$f_z^*(\varphi) = \frac{f_z(\varphi)}{f_{z_0}} - 1 - g_{\max} \leq 0, \tag{9}$$

where m_{z_0} and f_{z_0} are the values of f_z and f_z, respectively, calculated at the beginning of each iteration. The quantity $g_{\max}$ is the value of the largest constraint corresponding to the

design variable vector φ and is a constant for a particular iteration. Due to the fact that these reduced objective functions are analogous to the previous constraints, a new constraint vector $g_{2k}(\varphi)$, $k = 1, 2, \ldots, K$, is introduced, where K = NCON + NOBJ. The new objective function to be minimized is then defined, using the K-S function as follows:

$$F_2(\varphi) = g_{2_{max}} + \frac{1}{\rho} \log_e \sum_{k=1}^{K} \exp[\rho(g_{2_k}(\varphi) - g_{2_{max}})] \tag{10}$$

where the multiplier ρ can be considered analogous to a draw-down factor with ρ controlling the distance from the surface of the K-S objective function to the surface of the maximum function value.

RESULTS

The optimization procedure is applied to a wind tunnel model of the Growth Black Hack rotor blade which has a radius, R = 4.685 ft and a rotational velocity, Ω = 639.5 r.p.m. The rotor is in forward flight with and advance ratio, $\mu = 0.3$. The blade is discretized into 10 segments (i.e., NSEG = 10). Therefore, for the Min $\Sigma\beta$ approach a total of 34 design variables are used including the two pseudo design variables β_1 and β_2. For the K-S function approach, a total of 32 design variables (NMEM = 5, in Figure 1) are used. For convenience, the following notations will be used hereafter, the Min $\Sigma\beta$ approach will be referred to as Case I, and the K-S function approach will be referred to as Case II.

The optimum results are summarized in Tables 1 and 2 and Figures 5–9. Table 1 presents a summary of the important results. Substantial reductions are obtained in the objective function values. The 4/rev vertical shear (f_z) is reduced by 14.9 percent in Case I and by 17.6 percent in Case II. The 4/rev lagging moment (m_z) is reduced by 4.4 and 2.1 percent for Cases I and II, respectively (Table 1). The constraints for both cases are all satisfied. It is important to note that the coefficient of total power (C_p) is reduced by 4.3 percent for both cases, and represents a significant increase in economic efficiency in the optimum rotor. The thrust (T) is at the prescribed lower bound in Case I and is slightly increased (less than 1 percent) in Case II, guaranteeing at least the same lifting capability as the reference rotor. For the autorotational inertia (AI), the situation is reversed, with Case I yielding a slight increase (again less than 1 percent) and the constraint is critical in Case II. In Case I, the 3/rev radial and in-plane shears (f_r and f_x, respectively) and the 3/rev flapping moment (m_x) are all reduced by about 4 percent and the 3/rev torsional moment (m_c) is critical. In Case II, f_x is held at its upper bound, and f_r and m_x are reduced by 5.6 and 5.4 percent, respectively. The 3/rev vibratory torsional moment (m_c) is equal to the reference blade value for Case I, and is reduced by 2.9 percent Case II. The total weight (W) is also slightly reduced for both cases (less than 1 percent in Case I and 1.4 percent in Case II). It is interesting to note from Table 1, that the solidity, σ, of both the optimum rotors is close to the reference rotor (very marginal decrease) although the solidity was allowed to vary during optimization. Therefore the C_T/σ of both the optimum and reference rotors remains almost the same (the optimum rotors have a slightly higher value). Figure 5 more clearly depicts the significant reductions in the normalized objective functions (f_z and m_z) and the total power coefficient (C_p). The large reductions in C_p can be attributed to the inclusion of aerodynamic design variables, particularly the twist distribution.

Table 2 and Figures 7 and 8 present the design variables, before and after optimization. Table 2 shows that in both cases the optimum blade has a larger root chord (c_r) and is slightly tapered ($\lambda = 0.96$ and 0.94 for Cases I and II, respectively). The chord shape parameters α and p are nearly equal to the reference values for Case I (the Min $\Sigma\beta$ approach), whereas in Case II (the K-S function case), α experiences a 14 percent increase and p is similarly reduced by 12 percent. For Case I, the root twist (θ_r) is reduced by 1.7 percent and the twist ratio (τ) is increased by 7.8 percent (from reference blade) yielding a twist distribution that is nearly linear with a shape parameter $\delta = 0.957$ (see Figure 4). As indicated in Table 2, Case II produces very similar results, however in this case θ_r is increased by 1.5 percent and τ is reduced by 5.7 percent. The twist distribution is again close to linear with $\delta = 0.963$ (see Figure 4). The box beam wall

Table 1. Summary of optimum results.

		Reference blade	Bounds		Optimum	
			lower	upper	Min$\Sigma\beta$	K-S
Objective functions	4/rev f_z (lb)	0.201	-	-	0.171	0.166
	percent reduction				(14.9%)*	(17.6%)*
	4/rev m_x (lb-ft)	1.43	-	-	1.37	1.40
	percent reduction				(4.40%)*	(2.1%)*
Constraints	AI (lb-ft^2)	18.4	18.4	-	18.5	18.4
	W (lb)	3.18	-	3.18	3.17	3.13
	3/rev f_r (lb)	0.515	-	0.515	0.496	0.486
	3/rev f_z (lb)	0.331	-	0.331	0.325	0.331
	3/rev m_c (lb-ft)	0.119	-	0.119	0.119	0.116
	3/rev m_x (lb-ft)	1.12	-	1.12	1.07	1.06
	Thrust, T (lb)	282.	282.	-	282.	283.
	C_p	0.00105	-	0.00105	0.00100	0.00100
	x_{e_1}	0.0137	0.0	-	0.0138	0.0182
	x_{e_2}	0.0137	0.0	-	0.0149	0.0136
	x_{e_3}	0.0137	0.0	-	0.0143	0.0143
	x_{e_4}	0.0137	0.0	-	0.0151	0.0144
	x_{e_5}	0.0137	0.0	-	0.0159	0.0159
Solidity	σ	0.116	-	-	0.115	0.114
Trim	C_T/σ	0.0591	-	-	0.0593	0.0592

* Percent reduction from reference value.

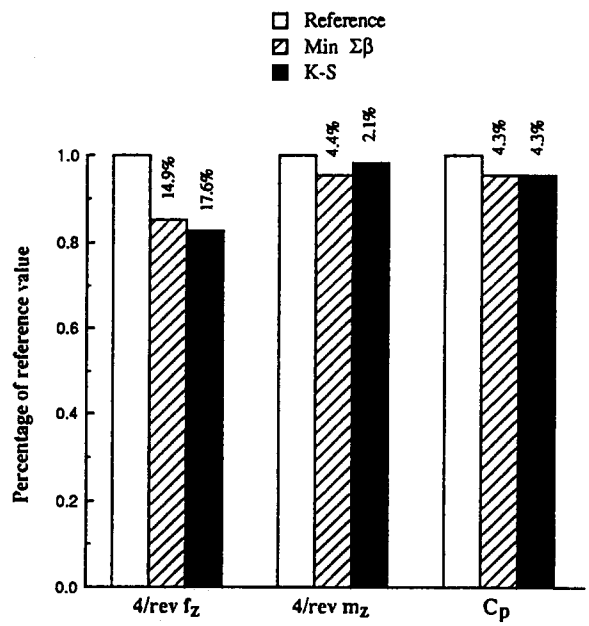

Figure 5. Comparisons of normalized vibratory loads and total power.

thicknesses demonstrate very different trends for the two cases. In Case I, the thicknesses of the upper and lower walls (t_4) and (t_5) increase by 4.2 and 6.1 percent respectively, whereas in Case II, t_5 increases substantially (23.4 percent), and t_4 reduces by 6.6 percent. Similarly, the vertical member nearest the leading edge, t_1, decreases by 2.9 percent in Case I and increases by 2.3 percent in Case II. The thickness, t_2 of the centrally located vertical member reduces marginally in Case I (less than 1.0 percent) and increases slightly (2.0 percent) in Case II. The thickness, t_3, of the aft vertical member is increased in both cases, although more dramatically

Table 2. Summary of design variables.

	Design Variables	Reference	Optimum	
			Min $\Sigma\beta$	K-S
Wall thickness at the root	t_{r_1} (in)	0.0312	0.0303	0.0319
	t_{r_2} (in)	0.0312	0.0311	0.0320
	t_{r_3} (in)	0.0312	0.0316	0.0349
	t_{r_4} (in)	0.0312	0.0325	0.0292
	t_{r_5} (in)	0.0312	0.0331	0.0386
Root chord	c_r (ft)	0.450	0.458	0.462
Chord shape parameters	λ	1.00	0.956	0.943
	α	0.0100	0.0101	0.0114
	p	0.0100	0.00984	0.00882
Root twist	θ_r (deg)	30.0	29.5	30.4
Twist shape parameters	τ	-0.333	-0.359	-0.314
	δ	1.00	0.957	0.963

in Case II (11.8 percent). Overall, the stiffness of the optimum blade in Case II is greater than the optimum blade in Case I, and both are greater than the reference blade at the root, as indicated through the torsional stiffness distribution in Figure 6. It should be noted that the total blade stresses $\sigma_{T_j}(j = 1, 2, \ldots, \text{NSEG})$, at each segment, were originally used as constraints, however, during optimization these constraints were well satisfied and were never active. Therefore, these were eliminated from the constraint vector. However, the stresses were computed after optimization to ensure that they remained well below the prescribed bounds.

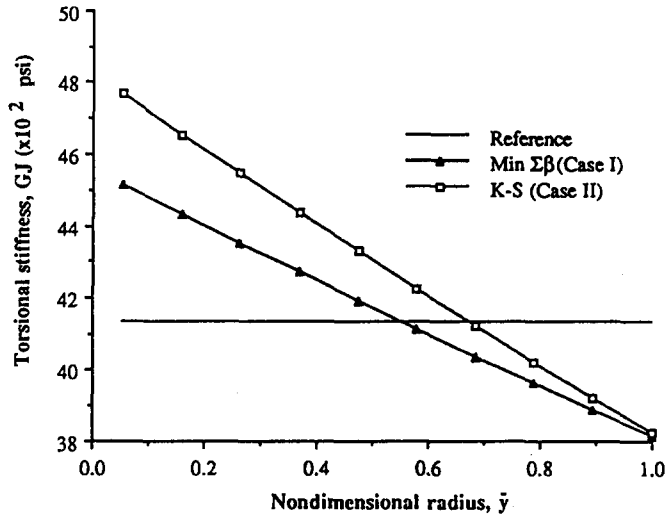

Figure 6. Blade stiffness distribution.

Figure 7 presents comparisons of the nonstructural weight distributions w_T (at leading edge) and w_c (at 35 percent chord). Using both multiobjective formulation procedures, similar trends are obtained in these w_t and w_c distributions. All of these distributions display reductions at inboard locations and increases towards blade outboard. However, the changes are more dramatic for Case II, especially for w_c. The trend can be explained as follows. In an effort to satisfy the autorotational inertia constraint while constraining the blade weight, the optimizer redistributes the weight such that the overall weight decreases whereas the outboard weights, which have larger effects on the blade autorotational inertia, increase. The large increases in the outboard nonstructural weights in Case II allow for similarly large decreases at blade inboard. This leads to a greater overall reduction in weight, as indicated in Table 1.

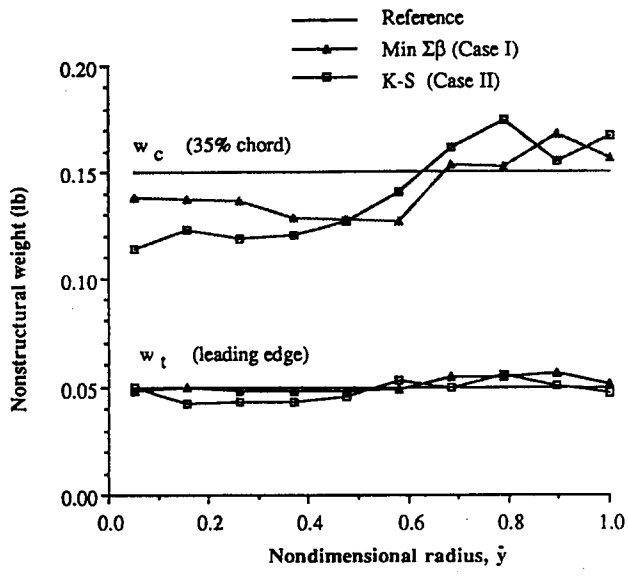

Figure 7. Blade nonstructural weight distribution.

The chord distributions of the reference and the optimum rotors are presented in Figure 8. The figure shows that the optimum blades both have slightly increased root chords and slightly tapered planforms. As indicated in the figure, the chord values at the tip are nearly identical to the reference blade, despite the fact that in Case II (the K-S function approach) there are significant changes in the tip shape parameters. This illustrates the fact that the root chord and taper ratio have more influence on the blade planform than the tip shape parameters α and p.

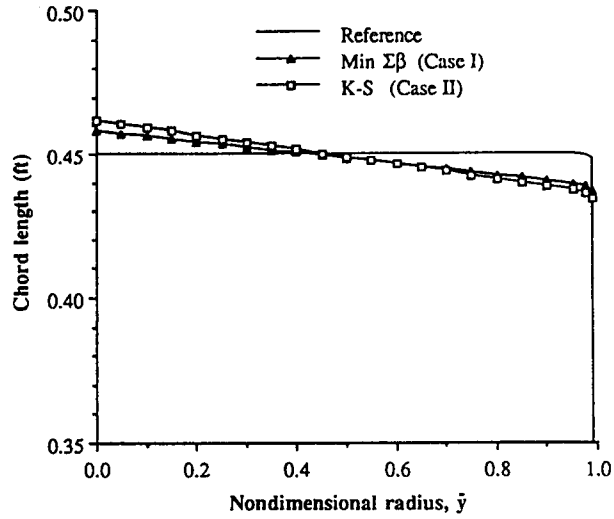

Figure 8. Chord distribution.

Figure 9 shows the center of gravity offset from the elastic axis (x_e) at discrete spanwise locations. The figure illustrates satisfactory values of x_e throughout the span for both cases. The center of gravity offsets are related to the distributions of the nonstructural weights. In both Cases I and II, the reductions in w_c are greater than the reductions in w_t at the inboard and midspan locations, which shifts the center of gravity forward and increases x_e. At the tip, the increase in w_c is greater than the increase in w_t thus shifting the center of gravity aftward and reducing x_e. Exceptions occurred at a few inboard locations where w_t reductions (from reference value) are significant and x_e is maintained near the reference values.

Figure 10 displays the convergence history of the objective functions used in the Min $\Sigma\beta$ and K-S function cases. The figure indicates that a smooth convergence is reached in Case I, (Min $\Sigma\beta$) in 15 cycles. This is expected since the objective function is strictly linear (equation (5)). However, in the K-S function approach (Case II) the convergence to optimum is highly nonlinear.

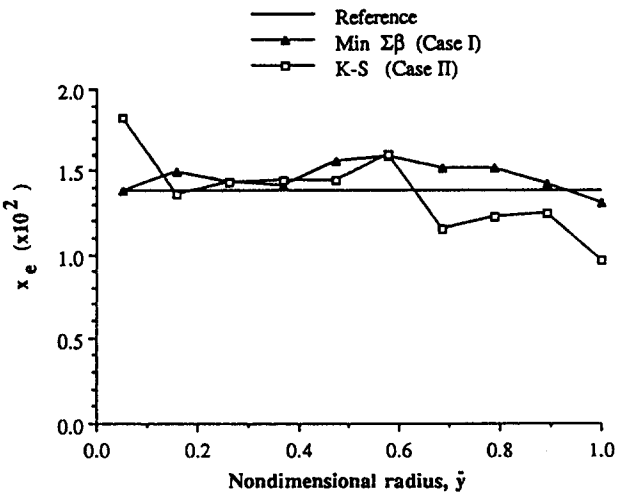

Figure 9. Blade center of gravity offset distribution.

This can be explained by noting that the value of the K-S function (equation (10)) is driven primarily by the largest violated constraint, g_{max}. Therefore, in an attempt to reduce the objective function, the optimizer would try to satisfy this constraint more vigorously than the others. Often, this leads to a new constraint for g_{max}, which, due to the nonlinearities of the rotor blade problem and the use of the approximate analysis, can be of the same order of magnitude that the previous g_{max} had been. Therefore, it is not unlikely that the convergence can be highly oscillatory.

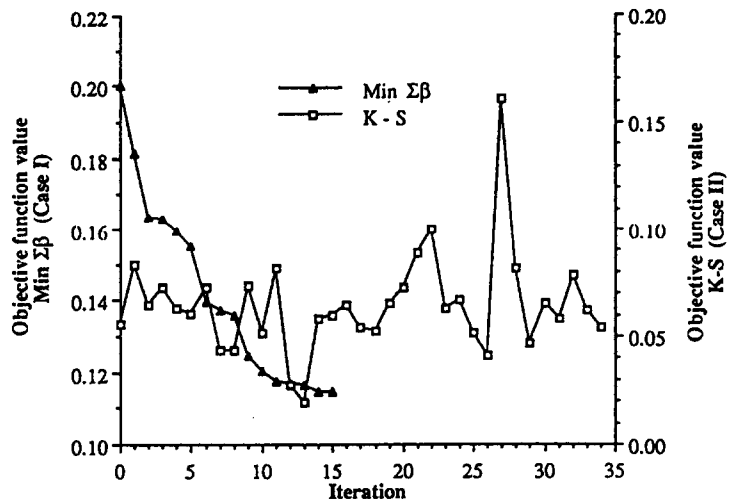

Figure 10. Objective function convergence history.

CONCLUDING REMARKS

This paper addresses the coupling of rotor dynamic, aerodynamic, structural and aeroelastic issues within a closed-loop optimization procedure. The 4/rev vertical shear and 4/rev lagging moments at the blade root are reduced with constraints imposed on the remaining critical vibratory forces and moments, rotor thrust, total power coefficient, autorotational inertia, blade weight, and the center of gravity—elastic axis offset. A two-celled box beam is designed as the principal load-carrying member inside the airfoil. Design variables include wall thicknesses of the box beam, magnitudes of the nonstructural weights located at the leading edge and at 35 percent chord (inside the box beam), chord and twist distributions. A Minimum Sum Beta (Min $\Sigma\beta$) and a Kreisselmeier-Steinhauser (K-S) function approach are used to formulate the multiobjective design problem. An existing blade model is used as a reference or baseline design. Optimum

designs for both cases are compared to the reference design. The following important observations are made.

(1) Significant reductions were obtained in both the objective functions using both multiobjective formulation procedures.
(2) The nonstructural weights, located at both leading edge (w_t) and at 35 percent chord (w_c), demonstrated similar trends of reduction at blade inboard locations, and increase towards outboard. This was due to the inclusion of weight and autorotational inertia constraints which are conflicting in nature.
(3) The stiffnesses of the optimum blade differed significantly from the reference due to the changes in the wall thicknesses of the box beam.
(4) The optimum chord distributions were tapered and the twist distributions were almost linear for both optimization formulation cases.
(5) The inclusion of the aerodynamic design variables provided significant reduction in the total power coefficient, C_p, in both cases.

References

1. J. Sobieszczanski-Sobieski, Ed., Recent experiences in multidisciplinary analysis and optimization, NASA CP-2327, (1984).
2. P.P. Friedmann, Application of modern structural optimization to vibration reduction in rotorcraft, *Vertica* **9** (4), 363–373 (1985).
3. H. Miura, Application of numerical optimization methods to helicopter design problems—A survey, *Vertica* **9** (2), 141–154 (1985).
4. R.B. Taylor, Helicopter vibration reduction by rotor blade modal shaping, In *Proc. of the 38th Annual Forum of the American Helicopter Society, Anaheim, California*, AHS, Washington, D.C., 90–101, (1982).
5. D.A. Peters, M.P. Rossow, A. Korn and T. Ko, Design of helicopter rotor blades for optimum dynamic characteristics, *Computers & Mathematics with Applications* **12A** (1), 85–109 (1986).
6. A. Chattopadhyay and J.L. Walsh, Minimum weight design of rectangular and tapered helicopter rotor blades with frequency constraints, *Journal of the American Helicopter Society*, 77–83 (October, 1989).
7. A. Chattopadhyay, and J.L. Walsh, Minimum weight design of rotorcraft blades with multiple frequency and stress constraints, *AIAA Journal* (March), 565–567 (1990).
8. P.P. Friedmann and P. Shantajumaran, Aeroelastic tailoring of rotor blades for vibration reduction in forward flight, In *AIAA SDM Conference*, Lake Tahoe, NV, Vol. 2, pp. 344–359, (May 1983).
9. S. Hanagud, A. Chattopadhyay, Y.K. Yillikci, D. Schrage and G. Reichert, Optimum design of a helicopter rotor blade, In *Proc. of the 12th European Rotorcraft Forum*, Paper No. 12, Garmisch-Partenkirchen, West Germany, (1986).
10. R. Celi and P.P. Friedmann, Efficient structural optimization of rotor blades with straight and swept tips, In *Proc. of the 13th European Rotorcraft Forum*, Arles, France, Paper No. 3-1, (1987).
11. J.W. Lim and I. Chopra, Aeroelastic optimization of a helicopter rotor, In *Proc. of the 44th Annual Forum of the AHS*, Washington, D.C., 545–558, (1988).
12. J.P. Magee, M.D. Maisel and F.J. Davenport, The design and performance of propeller/rotors for VTOL applications, In *Proc. of the 25th Annual AHS Forum*, (May 1981).
13. A. Chattopadhyay, J.L. Walsh and M.F. Riley, Integrated aerodynamic/dynamic optimization of helicopter blades, *Journal of Aircraft* **28** (1), 58–65 (January, 1991).
14. A. Chattopadhyay and Y.D. Chiu, An enhanced integrated aerodynamic load/dynamic optimization procedure for helicopter rotor blades, *Structural Optimization* **4**, 75-84 (1992).
15. C. He and D.A. Peters, Optimizatin of rotor blades for combined structural, dynamic, and aerodynamic properties, Presented at the *Third Air Force/NASA Symposium on Recent Advances in Multidisciplinary Analysis and Optimization*, San Francisco, CA, Sept. 24–26, (1990).
16. W.H. Weller and M.W. Davis, Applications of design optimization techniques to rotor dynamics problems, In *Proc. of the 42nd Annual Forum of the AHS*, June 2–4, pp. 27–44, (1986).
17. F. Straub, C.B. Callahan and J.D. Culp, Rotor design optimization using a multidisciplinary approach, Presented at the *29th Aerospace Sciences Meeting*, Paper No. AIAA 91-0477, Jan. 7–10, Reno, Nevada, (1991).
18. A. Chattopadhyay and T.R. McCarthy, Multiobjective design optimization of helicopter rotor blades with multidisciplinary couplings, In *Optimization of Structural Systems and Industrial Applications*, (Edited by S. Hernandez and C.A. Brebbia), pp. 451–462, (1991).
19. W. Johnson, A comprehensive analytical model of rotorcraft aerodynamics and dynamics, Part II: User's Manual, NASA TM-81183, (1980).
20. G.N. Vanderplaats, CONMIN—A Fortran program for constrained function minimization, User's Manual, NASA TMX-62282, (1973).

21. J. Sobieszczanski-Sobieski, A. Dovi and G. Wrenn, A new algorithm for general multiobjective optimization, NASA TM-100536, (March 1988).
22. W. Yeager, W. Mantay, M. Wilbur, R. Cramer and J. Singleton, Wind tunnel evaluation of an advanced main rotor blade design for a utility class helicopter, NASA TM-89129, (1987).